Supporting Information

Efficient Separation of Xylene Isomers by a Robust Calcium-Based Metal-Organic Framework through Synergetic Thermodynamically and Kinetically Controlled Mechanism

Yuhan Lin,[‡a] Jian Zhang,[‡a] Haardik Pandey,[‡b] Xinglong Dong,[c] Qihan Gong,[d] Hao Wang,*[a] Liang Yu,[a] Kang Zhou,[a] Wei Yu,[a] Xiaoxi Huang,[a] Timo Thonhauser,[b] Yu Han,*[c] and Jing Li*[e,a]

[a]Hoffmann Institute of Advanced Materials, Shenzhen Polytechnic, 7098 Liuxian Blvd., Nanshan District, Shenzhen, Guangdong 518055, China.

[b]Department of Physics and Center for Functional Materials, Wake Forest University, Winston-Salem, NC 27109, USA

[c]Advanced Membranes and Porous Materials Center, Physical Sciences and Engineering Division, King Abdullah University of Science and Technology
Thuwal 23955-6900, Saudi Arabia

[d]Fundamental Science & Advanced Technology Lab, PetroChina Petrochemical Research Institute, Beijing 102200, P. R. China

[e]Department of Chemistry and Chemical Biology, Rutgers University, 123 Bevier Road, Piscataway, New Jersey 08854, United States

Materials and characterization: All reagents were obtained from commercial sources and used without further purification. Powder X-ray diffraction patterns were recorded on a Bruker D8 Advance with Cu Kα radiation (λ= 1.5406 Å). Data were collected at room temperature at 2θ = 5-40°. Thermogravimetric analysis was carried out on a TGA550 (TA Instruments) analyzer. For each run 3-4 mg of sample was heated from room temperature to 600 °C at a ramp rate of 10 °C/min. Nitrogen adsorption at 77 K was measured on a Micromeritics 3Flex analyzer, and vapor adsorption experiment was conducted on a Belsorp-max II analyzer and a home-made gravimetric adsorption analyzer modified from a TGA55 (TA Instruments) unit. Single-crystal X-ray diffraction data were collected on a Bruker APEX-II CCD diffractometer using GaKα radiation tuned to λ = 1.34139 Å. The structure was solved by direct methods and refined by full-matrix least-squares on F^2 using the Bruker SHELXTL package.

Synthesis of HIAM-201: CaCl2 (50 mg) and H_4tcpp (50 mg) were added to 10 mL of ethanol (95%) and the mixture was stirred at room temperature for 2 hours before being transferred to a 20 mL Teflon bomb. The bomb was placed at an oven preset at 120 °C for 2 days. Colorless crystals were obtained after the reaction was cooled to room temperature (Yield: 70 % based on the organic ligand).

Multicoponent column breakthrough measurements: Column breakthrough measurement was performed with a lab-scale fix-bed reactor at 150 °C. In a typical experiment, 0.20 g of MOF material was packed into a quartz column (5.8 mm I.D. ×150 mm) with silane treated glass wool filling the void space. A helium flow (20 mL/ min) was used to purge the adsorbent. The MOF powder was activated at 150 °C overnight and the flow of helium was then turned off while another dry helium flow at a rate of 20 mL/min was bubbled through a mixture of xylene isomers with predetermined volumes (the volumes were determined through trial and error and calculated by GC: the experiment was run without any sample and the vapor phase ratios were optimized to an equimolar mixture). The effluent from the column was monitored using an online GC equipped with HP-PONA column and FID.

Single-component vapor adsorption measurements: Single-component adsorption isotherms of pX, mX, and oX at 120-150 °C were collected by a Belsorp-Max II volumetric adsorption analyzer. For each run, ~ 150 mg of HIAM-201 sample was activated at 150 °C under vacuum prior to adsorption measurements. The isotherms were collected from 0.001 kPa to 1.2 kPa. Adsorption rates were measured on a home-modified gravimetric adsorption analyzer adapted from a TGA55 (TA Instruments) unit. Around ~20 mg of HIAM-201 was used and activated at 150 °C overnight under nitrogen flow. After activation, the nitrogen flow was switched to another nitrogen flow bubbled from a bubbler containing xylene isomers. The partial pressure of the adsorbate vapor was adjusted by the vapor flow rate and the other nitrogen flow rate. The sample weight was monitored throughout the experiments.

Computational calculations. The HIAM-201 structure, shown in Figure 1, was used for our theoretical study, with 121 atoms included per unit cell. All *ab initio* calculations were performed using density functional theory (DFT), with the help of VASP (Vienna Ab Initio Simulation Package)[1-2] along with the vdW-DF functional.[3-6] Spin-polarized calculations were carried out, due to presence of N atoms in the MOF cell. The plane-wave energy cut-off was set at 600 eV and the SCF convergence condition was set to be 10^{-2} meV. The unit-cell parameters were varied in all directions during relaxation in order to achieve an optimal cell volume and shape. The MOF structure was optimized until all forces between atoms were smaller than 5 meV/Å. For binding-energy calculation, the guest molecules (m-xylene, o-xylene) were placed in the MOF pores at various sites and all the atoms were

allowed to relax until the convergence condition was reached. The total energy of the optimized MOF structure and the guest molecule configurations were used to calculate the corresponding binding energies. Induced charge densities were also calculated, showing the rearrangement of charge density upon bringing the guest molecules into the MOF and help identifying the interactions at the binding sites.

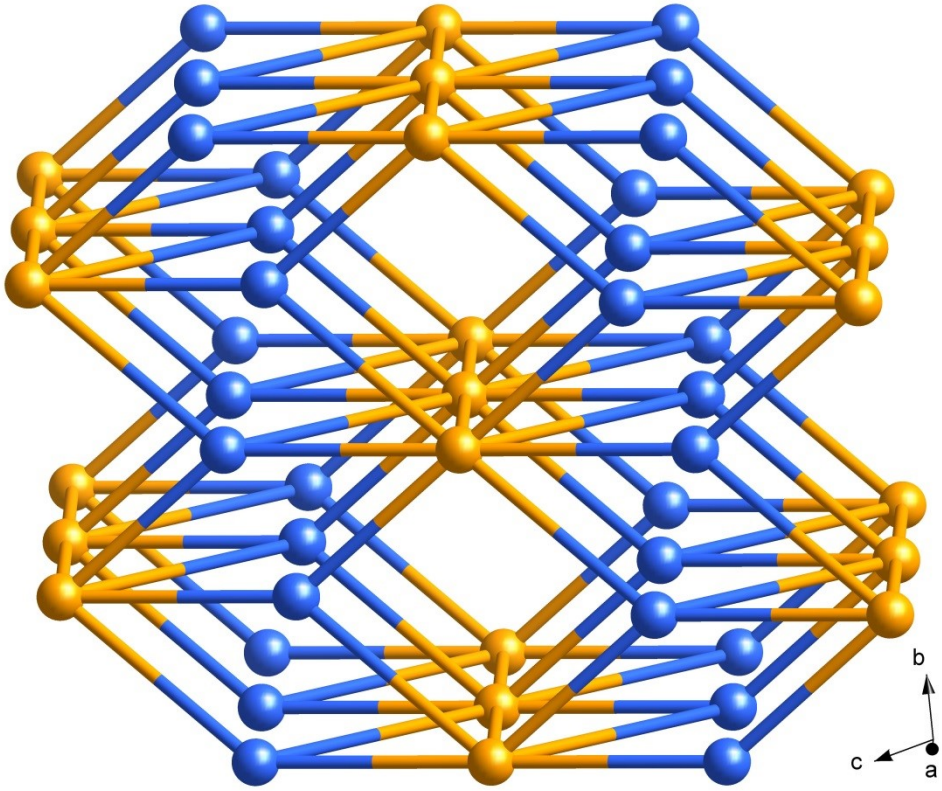

Fig. S1. Topology presentation of HIAM-201 (deh1 topology). Gold and blue balls represent Ca(II) centers and the tetra topic ligands, respectively.

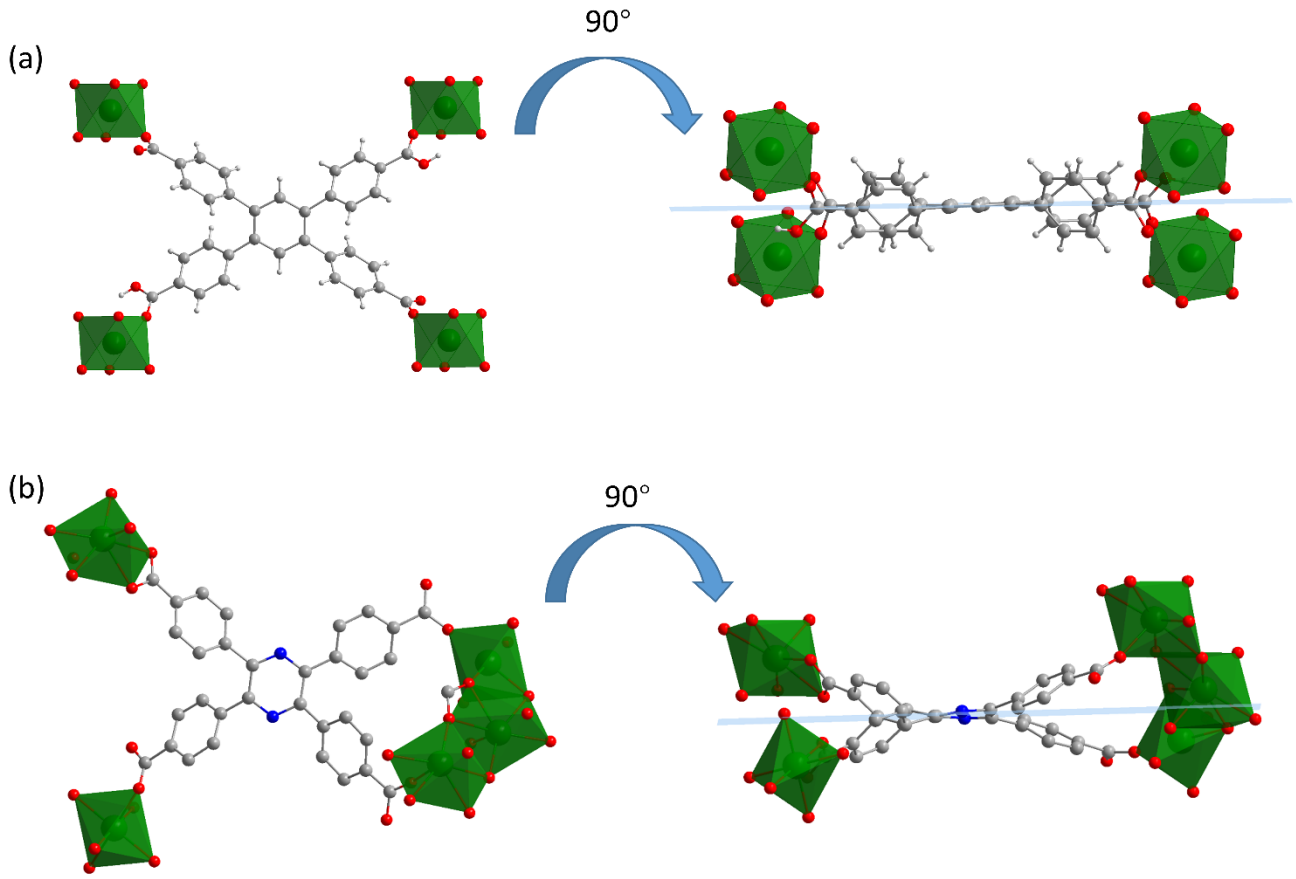

Fig. S2. Comparison of the configuration of the ligands in Ca(H_2tcpb) (a) and HIAM-201 (b).

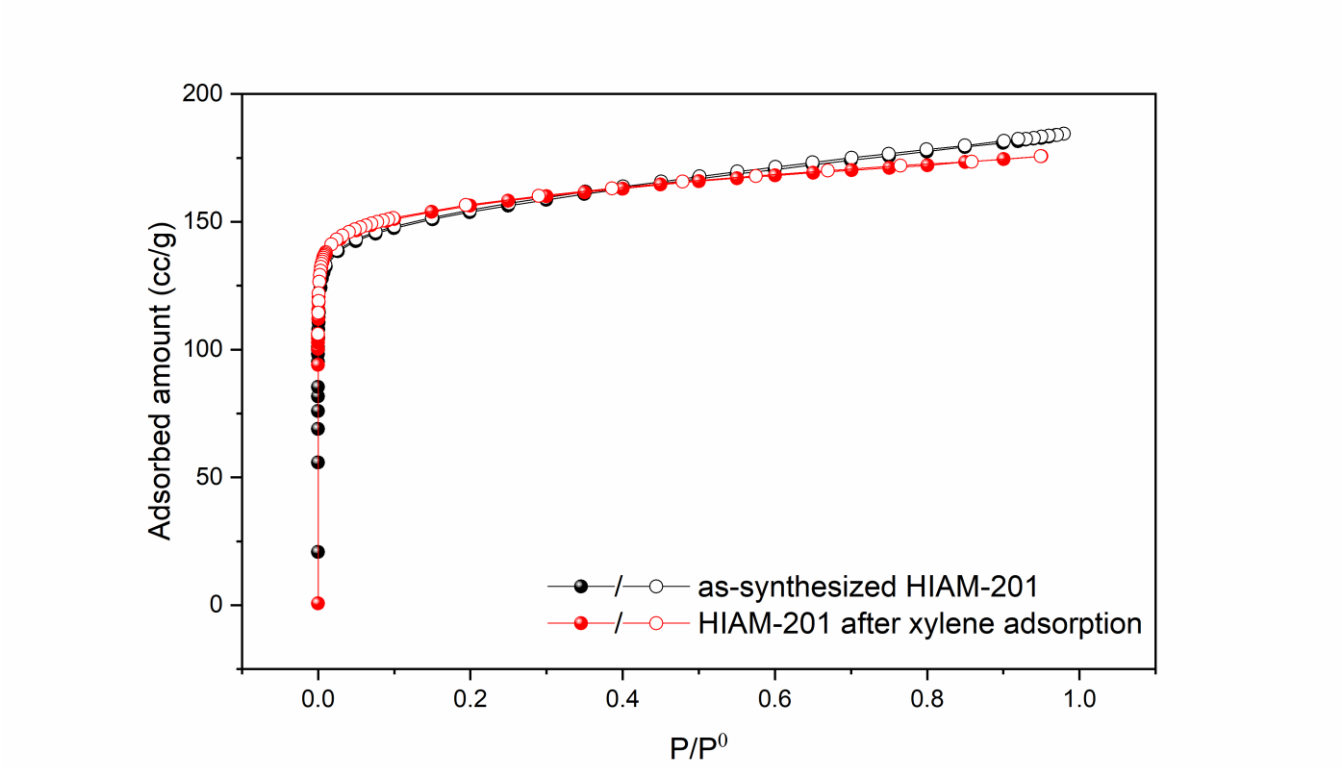

Fig. S3. Nitrogen adsorption isotherm on HIAM-201 at 77 K.

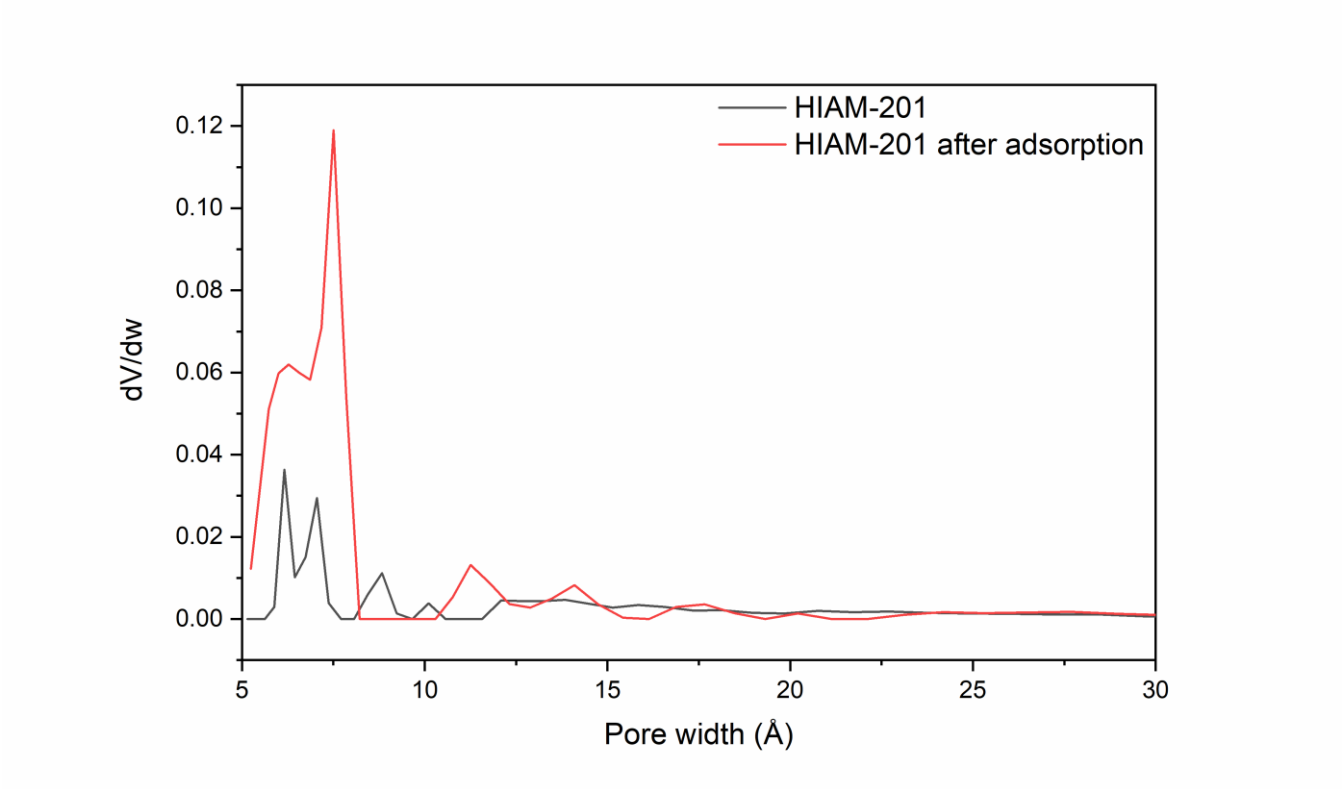

Fig. S4. NLDFT pore size distribution of HIAM-201 calculated from N2 adsorption at 77 K.

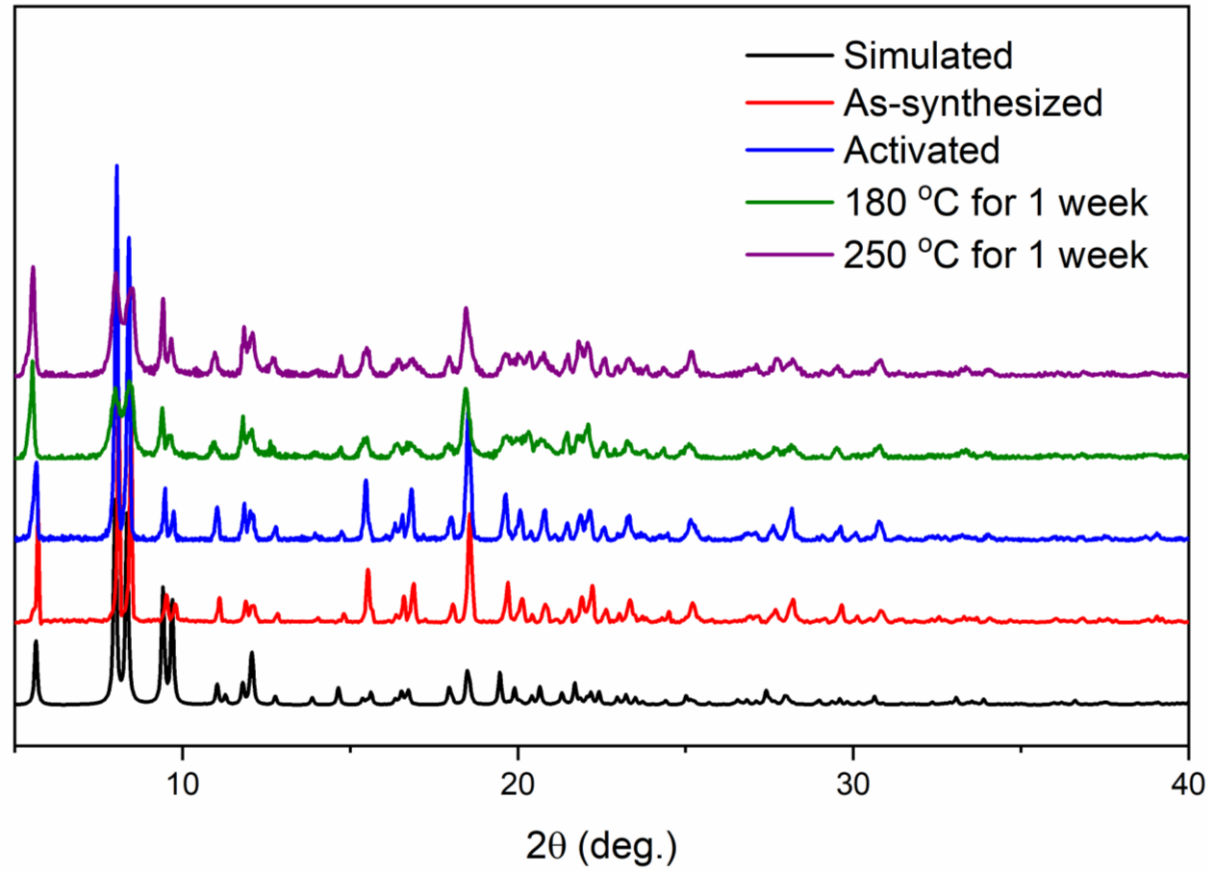

Fig. S5. PXRD patterns of HIAM-201 under various conditions.

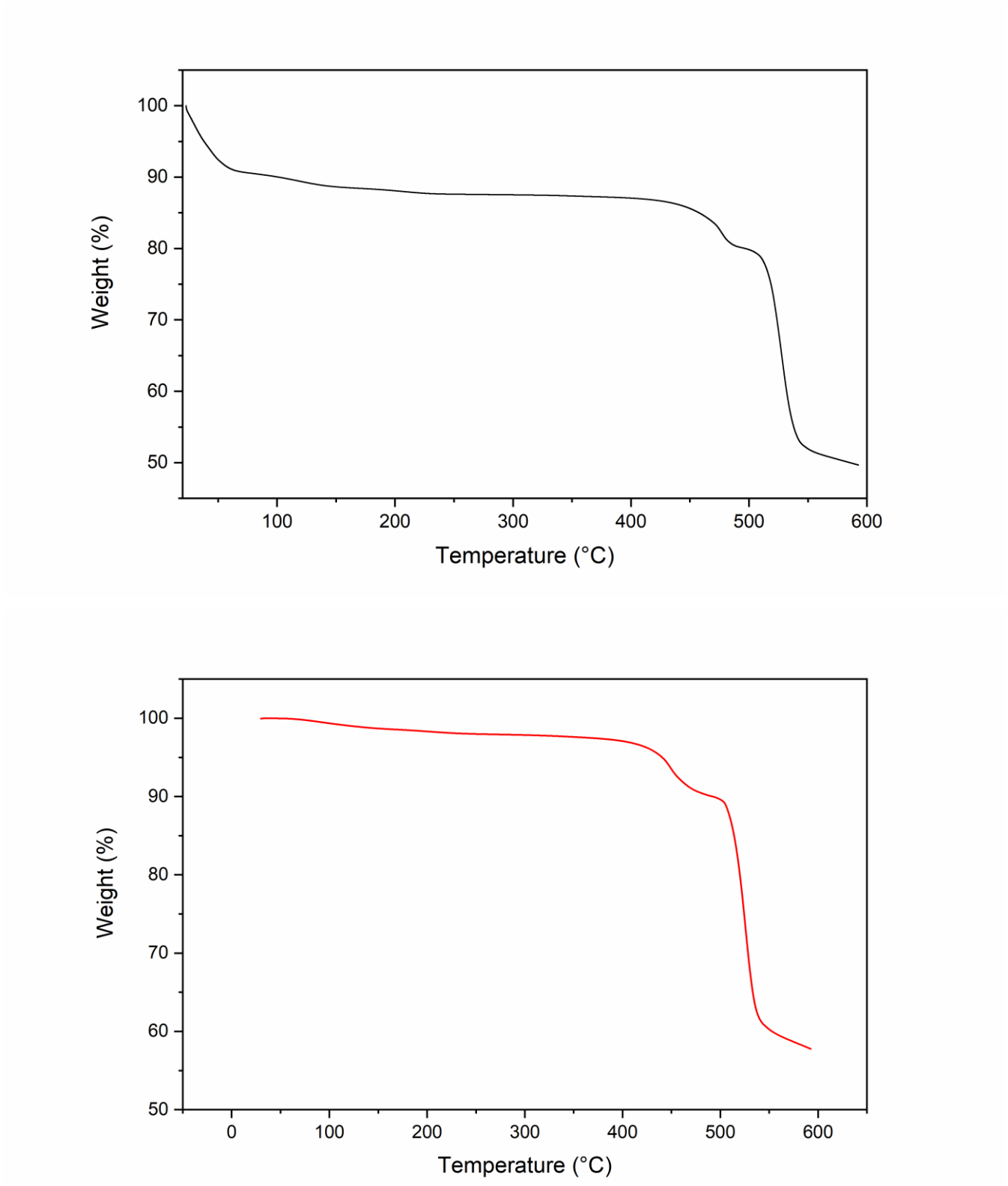

Fig. S6. TG profile of the as-synthesized (top) and activated (bottom) HIAM-201.

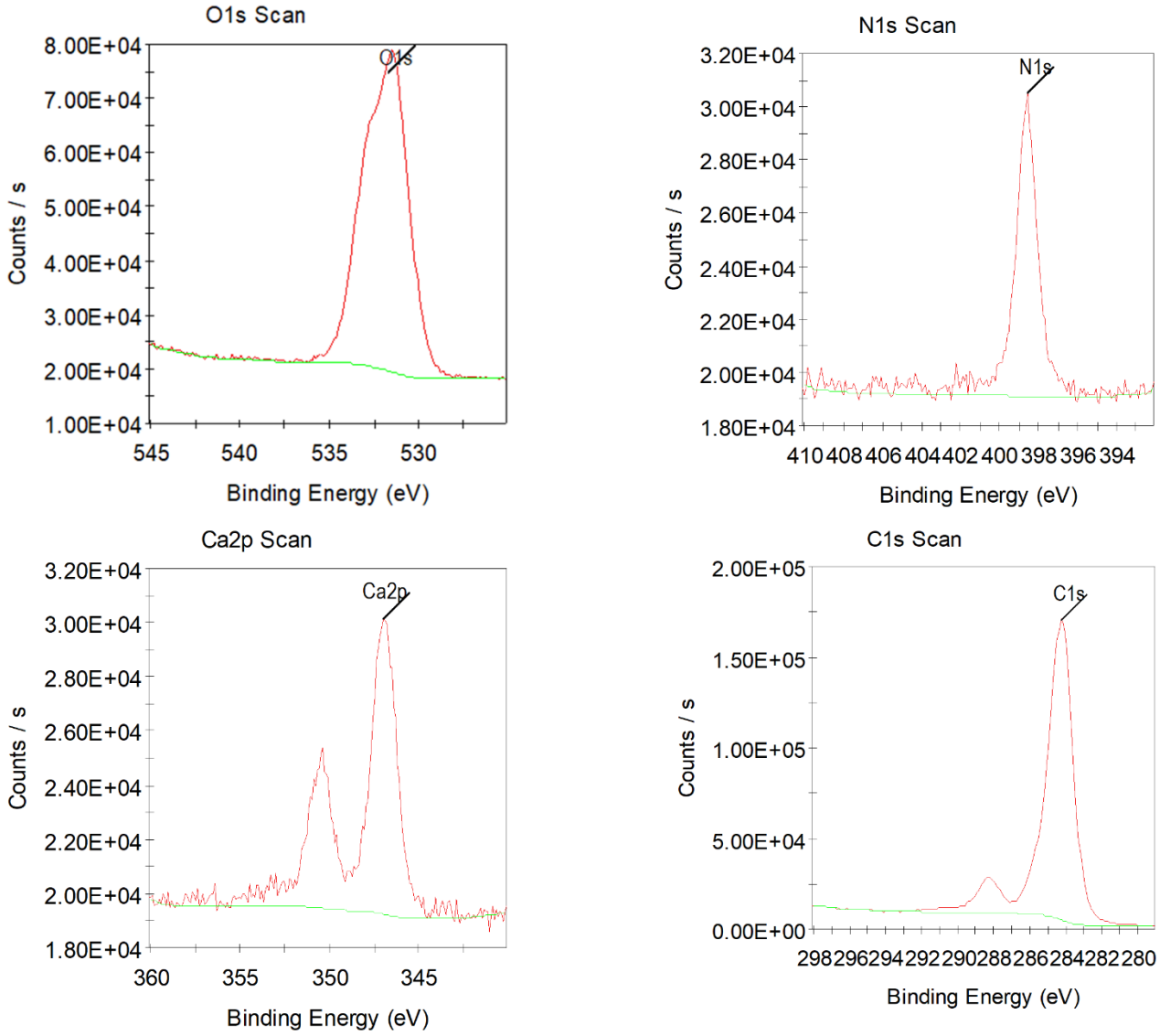

Fig. S7. XPS results of the as-synthesized HIAM-201.

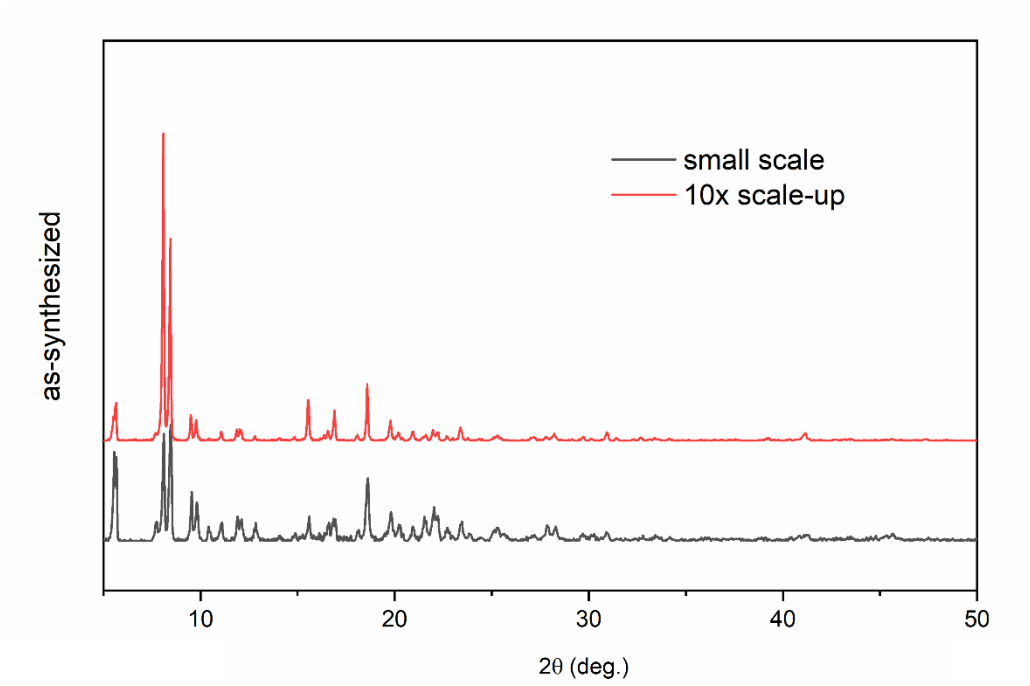

Fig. S8. PXRD patterns of the as-synthesized HIAM-201, small scale and 10x scale.

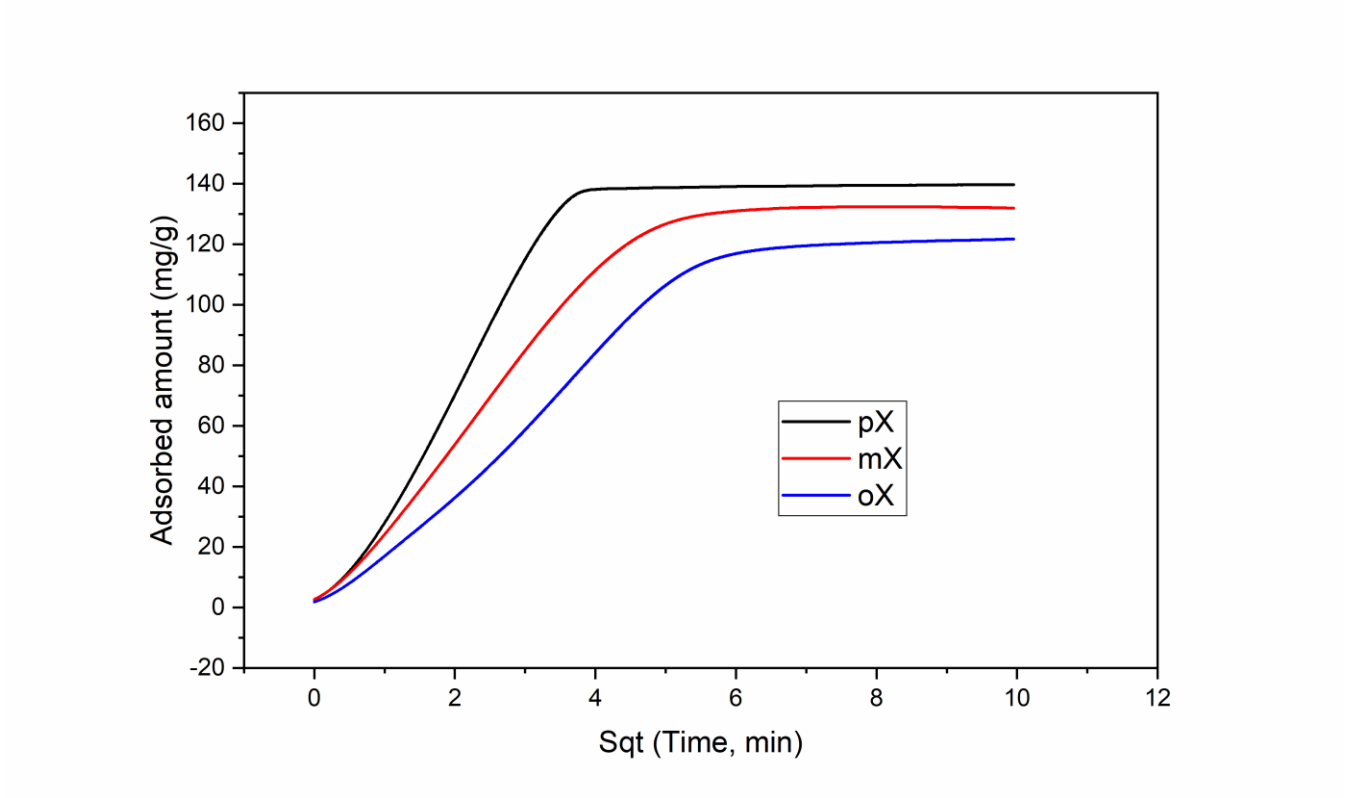

Fig. S9. Adsorption uptake of xylene isomers by HIAM-201 as a function of square root of time at 120 °C and 0.8 kPa.

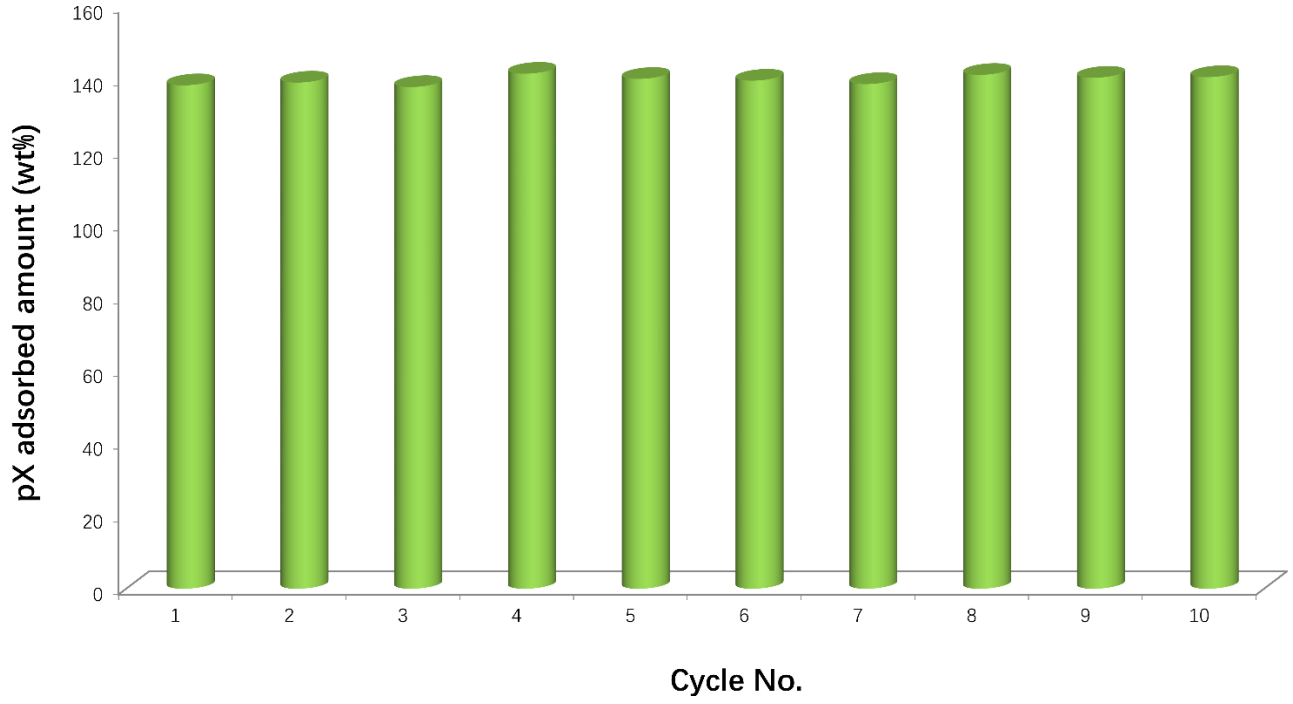

Fig. S10. 10 consecutive adsorption cycles of pX by HIAM-201 at 0.8 kPa and 150 °C

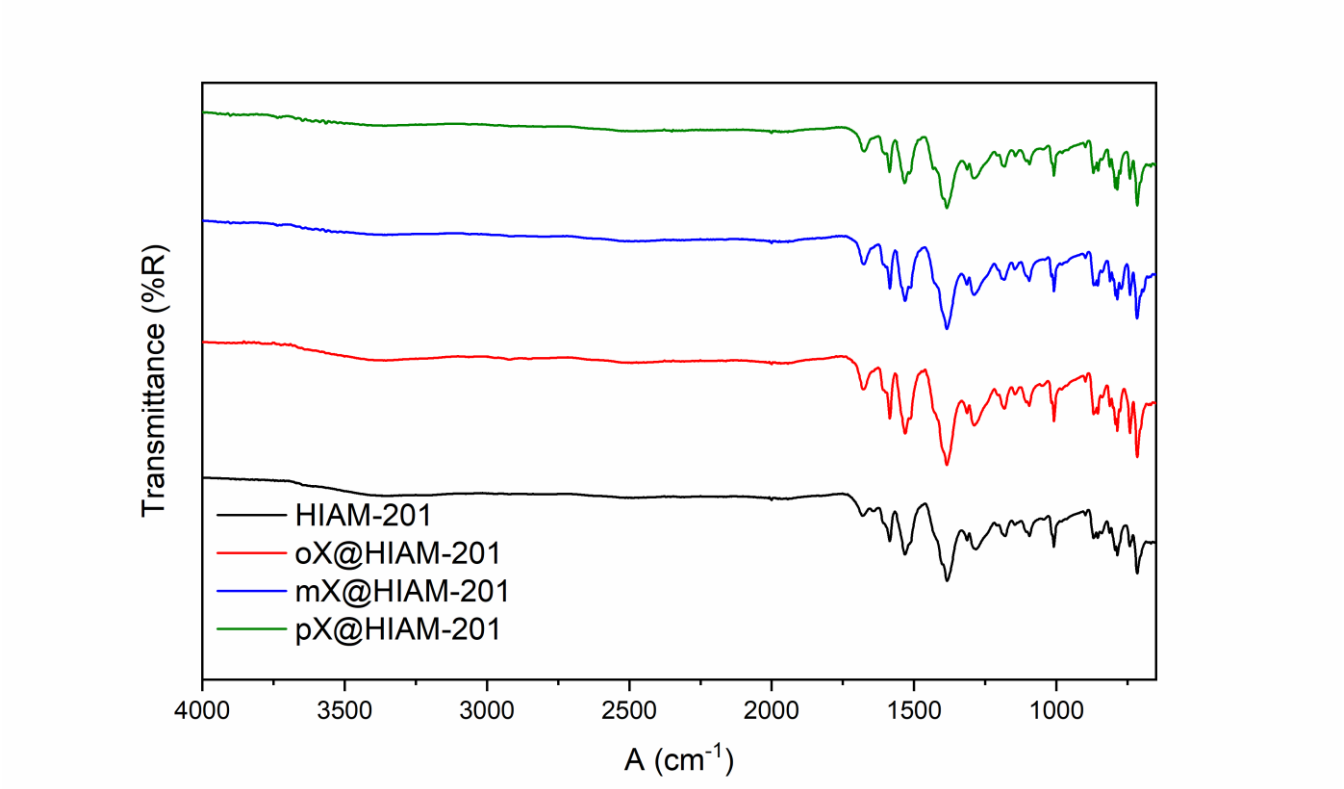

Fig. S11. IR spectra of HIAM-201 and xylenes loaded HIAM-201.

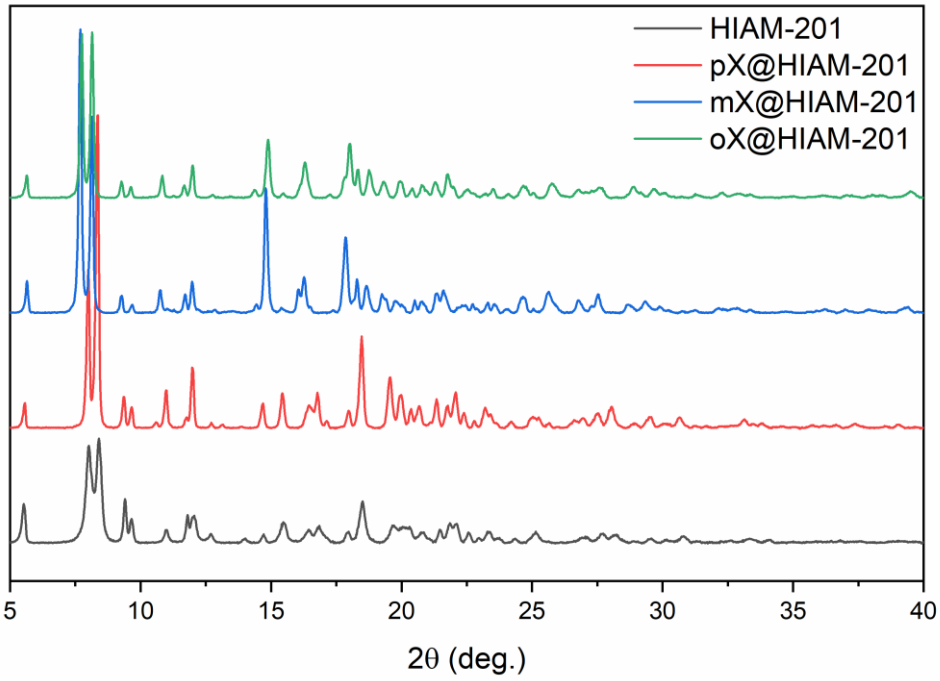

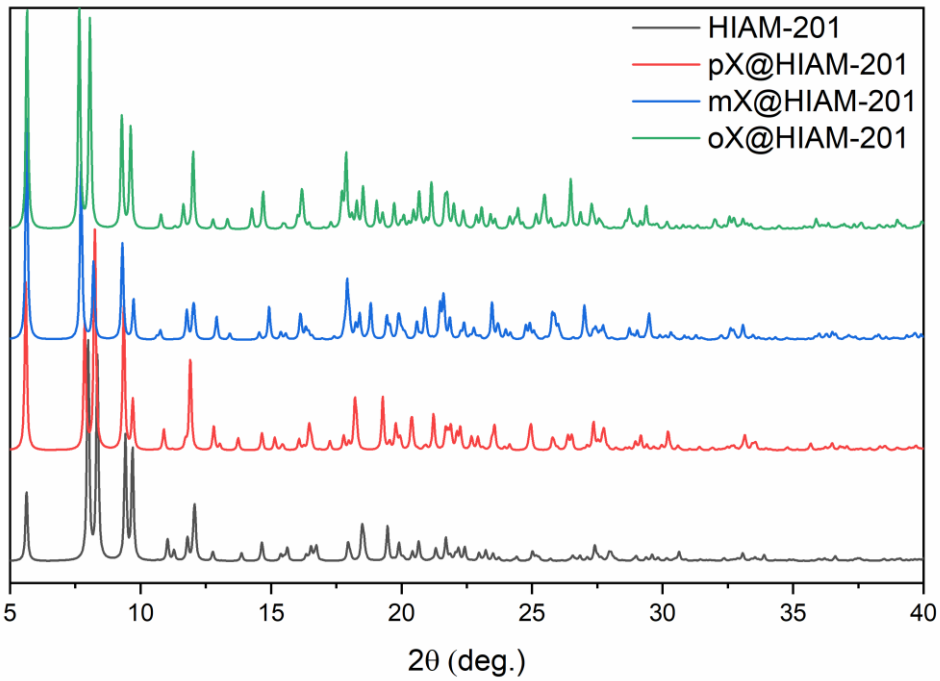

Fig. S12. Experimental (top) and simulated (bottom) PXRD patterns of HIAM-201 and xylenes loaded HIAM-201.

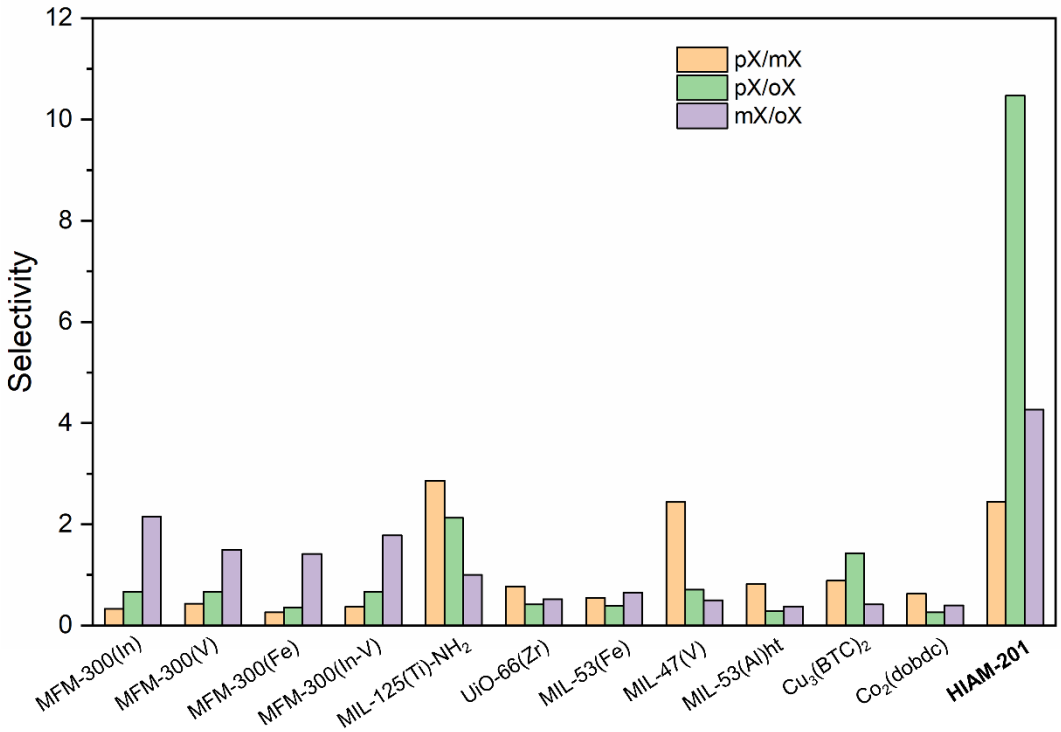

Fig. S13. Comparison of selectivity data calculated from breakthrough curves or from multicomponent liquid-phase adsorption experiments. (Data adapted from Ref. # 15 in the main text).

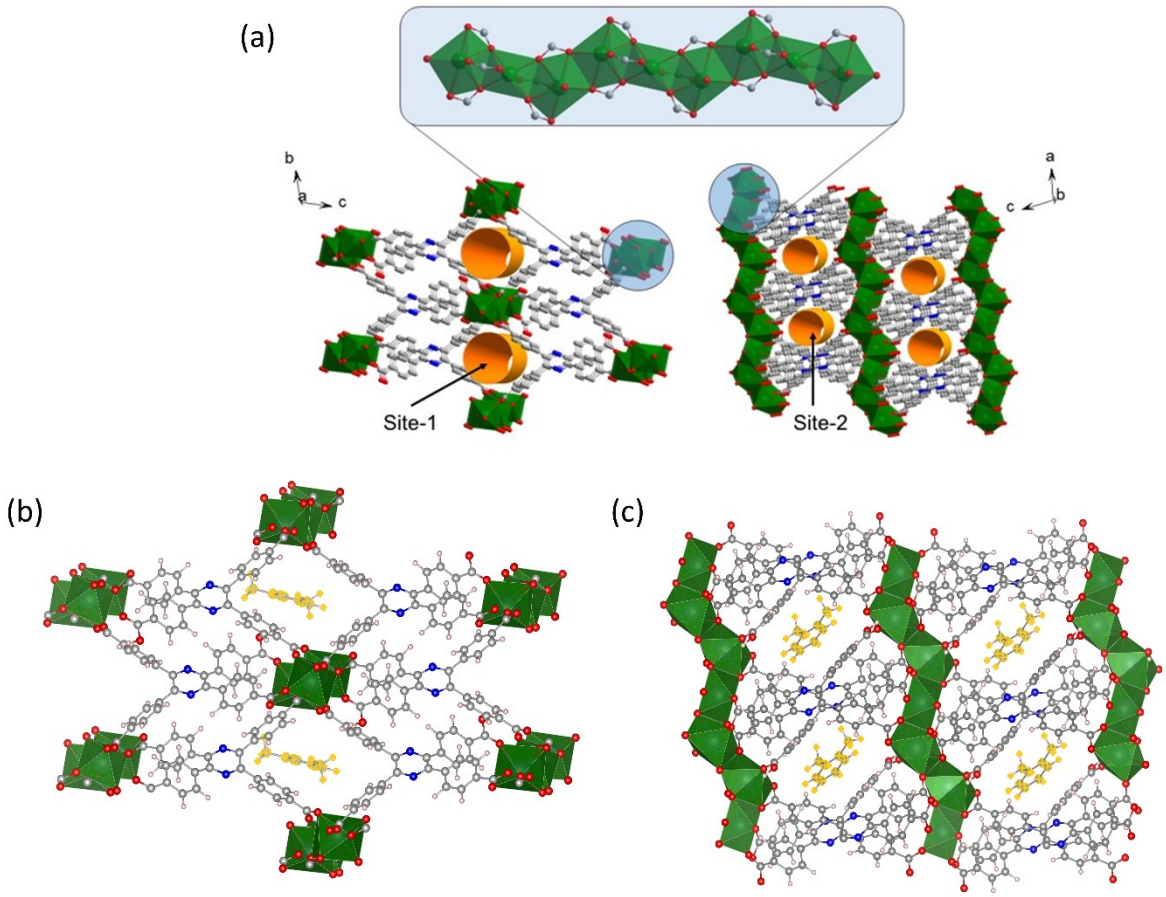

Fig. S14. Computational calculation results of (a) Two adsorption sites in two different channels of HIAM-201. (b) Preferential adsorption site of mX (site-1). (c) Preferential adsorption site of oX (site-2).

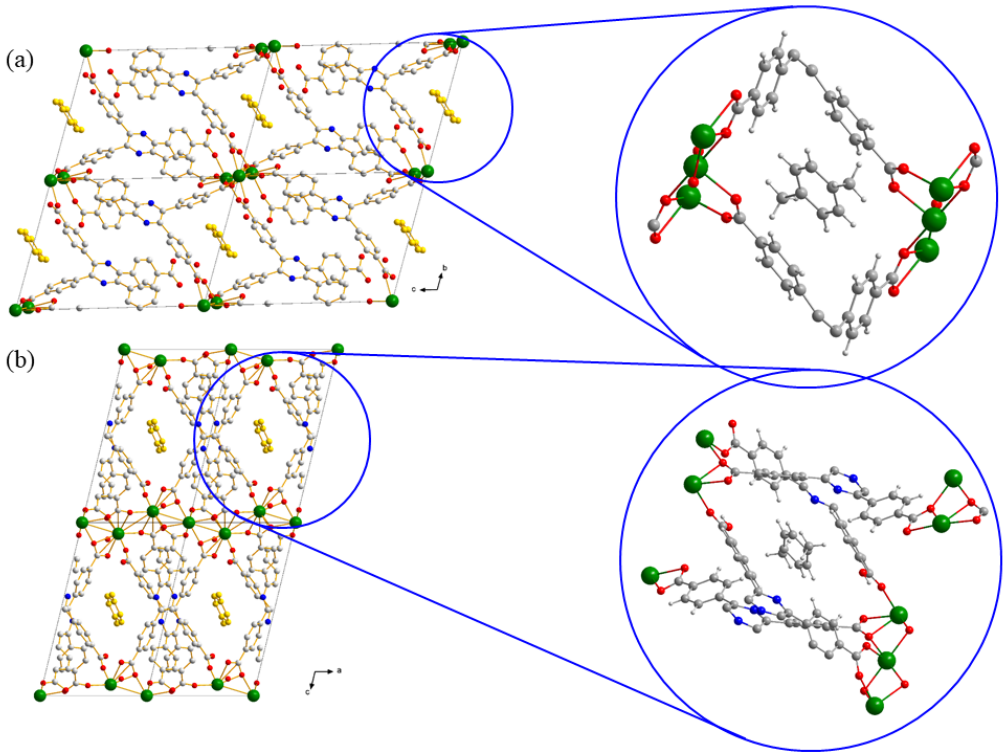

Fig. S15. Crystal structure of pX@HIAM-201 and the position of pX in two different channels.

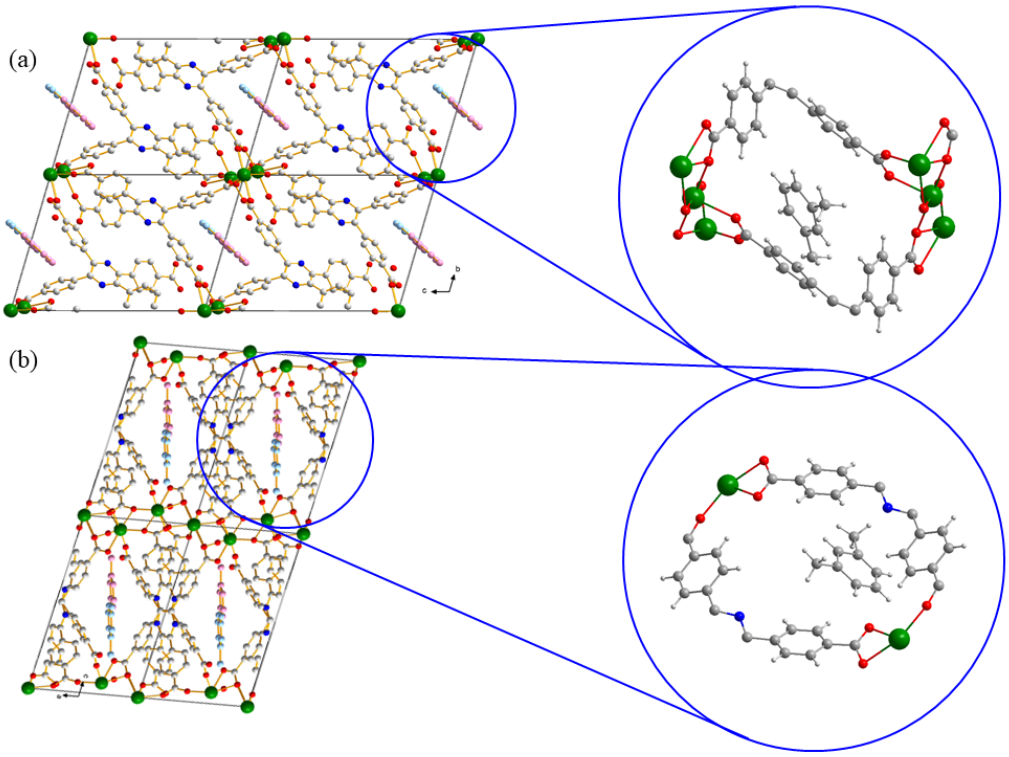

Fig. S16. Crystal structure of mX@HIAM-201 and the position of mX in two different channels.

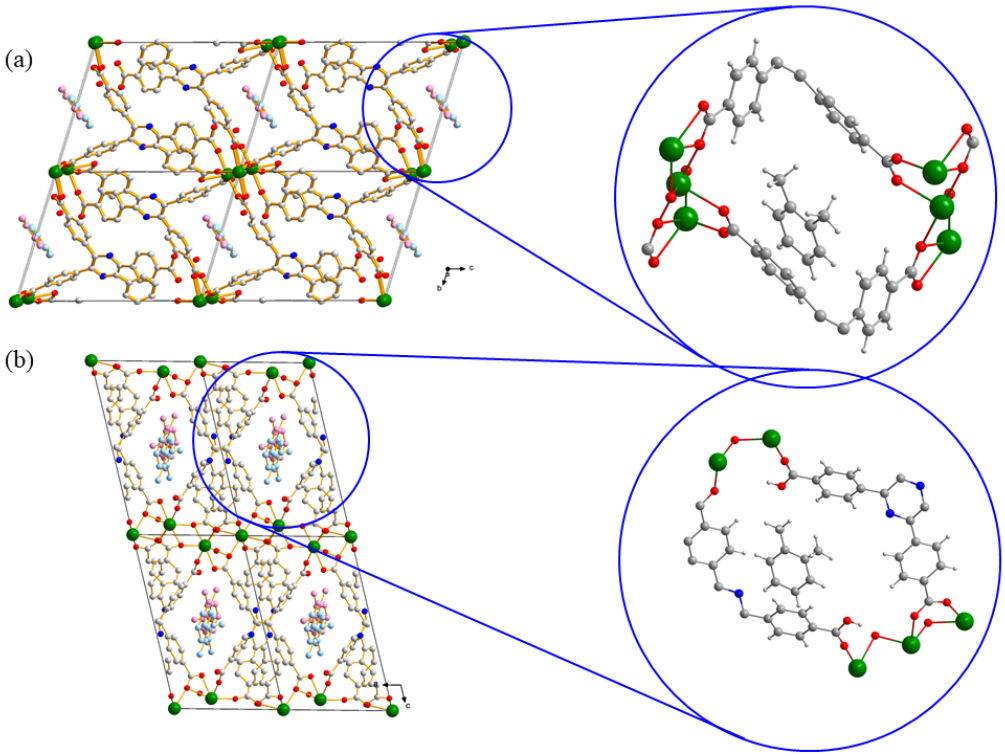

Fig. S17. Crystal structure of oX@HIAM-201 and the position of oX in two different channels.

Table S1. Summary of reported 3D Ca-MOFs with permanent porosity (measured BET surface area > 50 m^2/g). (Adapted from Ref #16 in the main text)

Name	Formula	BET surface area (m^2/g)
Ca-SBF	[Ca2(SBF-TCA)(DMF)2]	378
Ca-SBF-1	[Ca2(SBF-TCA) (CH3OH)2(H2O)2]	444
UTSA-280/Ca(squarate)	Ca(squarate) (H2O)	224/331
SBMOF-1/CYCU-1	Ca(SDB)	224/145
SBMOF-2	Ca(H2TCPB)	195/200
CaBTB	[Ca5(BTB)2(HBTB)2(H2O)6]	914
MOF-1201	Ca14(l-LAC)20(acetate)8(C2H5OH)(H2O)	430
MOF-1203	Ca6(l-LAC)3(acetate)9(H2O)	160
/	(H3O+)2[Ca(NDA)(C2H5O)(OH)]4 · 1 · 1H2O	353
/	[Ca4(BDC-F4)4(H2O)4] · 4H2O	348
/	Ca6(1,3-ADC)4(CO3)(OH)2(H2O)14	180
HIAM-201	**$Ca_3(Htcpp)_2$**	**640**

Table S2. Henry Constants (mg/g/kPa) of the adsorption of xylene isomers on HIAM-201 (120 -150 °C).

	120 °C	130 °C	140 °C	150 °C
pX	1031.62	835.97	476.97	298.96
mX	512.95	353.16	110.10	60.98
oX	189.44	86.95	37.58	24.35

Table S3. Crystal data and structure refinement for HIAM-201.

Identification code	HIAM-201
Chemical formula	$C_{64}H_{34}Ca_3N_4O_{16}$
M_r	1235.19
Crystal system,	Triclinic
space group	*P*-1
Temperature (K)	296
a, *b*, *c* (Å)	9.8952 (15), 11.7893 (18), 16.671 (3)
a, b, g (°)	103.829 (5), 100.898 (5), 101.724 (5)
V (Å^3)	1790.4 (5)
Z	1
Radiation type	Mo *K*a
m (mm^{-1})	0.29
Crystal size (mm)	0.10 × 0.10 × 0.10
Diffractometer	Bruker D8 VENTURE dual wavelength Mo/Cu
T_{min}, T_{max}	0.299, 0.429
No. of measured, independent and observed [I > 2s(I)] reflections	5959, 5959, 4255
R_{int}	0.077
(sin q/l)$_{max}$ (Å^{-1})	0.595
$R[F^2 > 2s(F^2)]$, $wR(F^2)$, S	0.094, 0.242, 1.01
No. of reflections	5959
No. of parameters	396
H-atom treatment	H-atom parameters constrained
Dρ$_{max}$, Dρ$_{min}$ (e Å^{-3})	0.54, -0.69

Table S4. Crystal data and structure refinement for pX@HIAM-201.

Identification code	pX@HIam-201
Empirical formula	$C_{76}H_{47.5}Ca_3N_4O_{18}$
Formula weight	1424.92
Temperature/K	192.97
Crystal system	triclinic
Space group	P-1
a/Å	9.9450(4)
b/Å	11.9934(4)
c/Å	16.6979(6)
α/°	103.8040(10)
β/°	100.041(2)
γ/°	102.1880(10)
Volume/Å^3	1836.77(12)
Z	1
ρ_{calc}g/cm^3	1.288
μ/mm^{-1}	1.678
F(000)	736.0
Crystal size/mm^3	? × ? × ?
Radiation	GaKα (λ = 1.34139)
2Θ range for data collection/°	6.846 to 106.054
Index ranges	-11 ≤ h ≤ 11, -14 ≤ k ≤ 13, 0 ≤ l ≤ 19
Reflections collected	9742
Independent reflections	9742 [R_{int} = ?, R_{sigma} = 0.0402]
Data/restraints/parameters	9742/312/475
Goodness-of-fit on F^2	1.058
Final R indexes [I>=2σ (I)]	R_1 = 0.0593, wR_2 = 0.1664
Final R indexes [all data]	R_1 = 0.0678, wR_2 = 0.1764
Largest diff. peak/hole / e Å^{-3}	0.79/-0.52

Table S5. Crystal data and structure refinement for mX@HIAM-201.

Identification code	mX@HIAM-201
Empirical formula	$C_{80}H_{58}Ca_3N_4O_{18}$
Formula weight	1483.54
Temperature/K	192.97
Crystal system	triclinic
Space group	P-1
a/Å	9.912(2)
b/Å	12.109(3)
c/Å	16.558(4)
α/°	103.792(7)
β/°	99.934(7)
γ/°	100.425(8)
Volume/Å^3	1849.3(8)
Z	1
ρ_{calc}g/cm^3	1.332
μ/mm^{-1}	0.297
F(000)	770.0
Crystal size/mm^3	? × ? × ?
Radiation	MoKα (λ = 0.71073)
2Θ range for data collection/°	4.288 to 52.776
Index ranges	-12 ≤ h ≤ 12, -15 ≤ k ≤ 14, 0 ≤ l ≤ 20
Reflections collected	7354
Independent reflections	7354 [R_{int} = ?, R_{sigma} = 0.1038]
Data/restraints/parameters	7354/385/532
Goodness-of-fit on F^2	1.038
Final R indexes [I>=2σ (I)]	R_1 = 0.0804, wR_2 = 0.2265
Final R indexes [all data]	R_1 = 0.1199, wR_2 = 0.2619
Largest diff. peak/hole / e Å^{-3}	1.02/-0.66

Table S6. Crystal data and structure refinement for oX@HIAM-201.

Identification code	oX@HIAM-201
Empirical formula	$C_{80}H_{40}Ca_3N_4O_{18}$
Formula weight	1465.40
Temperature/K	192.97
Crystal system	triclinic
Space group	P-1
a/Å	9.9598(4)
b/Å	12.2596(5)
c/Å	16.6543(7)
α/°	104.7154(17)
β/°	100.9054(16)
γ/°	99.7692(18)
Volume/Å^3	1879.88(13)
Z	1
ρ_{calc}g/cm^3	1.294
μ/mm^{-1}	1.652
F(000)	752.0
Crystal size/mm^3	? × ? × ?
Radiation	GaKα (λ = 1.34139)
2Θ range for data collection/°	8.08 to 106.218
Index ranges	-11 ≤ h ≤ 11, -14 ≤ k ≤ 14, 0 ≤ l ≤ 19
Reflections collected	6504
Independent reflections	6504 [R_{int} = ?, R_{sigma} = 0.0337]
Data/restraints/parameters	6504/576/601
Goodness-of-fit on F^2	1.083
Final R indexes [I>=2σ (I)]	R_1 = 0.0459, wR_2 = 0.1390
Final R indexes [all data]	R_1 = 0.0493, wR_2 = 0.1424
Largest diff. peak/hole / e Å^{-3}	0.62/-0.48

References

1. Kresse, G.; Joubert, D., From ultrasoft pseudopotentials to the projector augmented-wave method. *Physical Review B* **1999,** *59*, 1758-1775.
2. Kresse, G.; Furthmüller, J., Efficient iterative schemes for ab initio total-energy calculations using a plane-wave basis set. *Physical Review B* **1996,** *54*, 11169-11186.
3. Thonhauser, T.; Zuluaga, S.; Arter, C. A.; Berland, K.; Schröder, E.; Hyldgaard, P., Spin Signature of Nonlocal Correlation Binding in Metal-Organic Frameworks. *Physical Review Letters* **2015,** *115*, 136402.
4. Thonhauser, T.; Cooper, V. R.; Li, S.; Puzder, A.; Hyldgaard, P.; Langreth, D. C., Van der Waals density functional: Self-consistent potential and the nature of the van der Waals bond. *Physical Review B* **2007,** *76*, 125112.
5. Langreth, D. C.; Lundqvist, B. I.; Chakarova-Käck, S. D.; Cooper, V. R.; Dion, M.; Hyldgaard, P.; Kelkkanen, A.; Kleis, J.; Kong, L.; Li, S.; Moses, P. G.; Murray, E.; Puzder, A.; Rydberg, H.; Schröder, E.; Thonhauser, T., A density functional for sparse matter. *Journal of Physics: Condensed Matter* **2009,** *21*, 084203.
6. Berland, K.; Cooper, V. R.; Lee, K.; Schröder, E.; Thonhauser, T.; Hyldgaard, P.; Lundqvist, B. I., van der Waals forces in density functional theory: a review of the vdW-DF method. *Reports on Progress in Physics* **2015,** *78*, 066501.